

Determination of elements in Hunza River sediment by k_0 instrumental neutron activation analysis

Mohammad Wasim · Sajid Iqbal · Mohammad Arif · Manzoor Ali

Received: 17 December 2012 / Published online: 26 March 2013
© Akadémiai Kiadó, Budapest, Hungary 2013

Abstract This paper presents elemental data of sediment samples and its analysis methodology. The samples were collected from Central Karakoram—an unexplored region in Pakistan. Surface sediment samples (0–10 cm) were collected from 9 different locations along the Hunza River in Central Karakoram at an average altitude of 1,561 m covering almost 100 km length along the river. Samples were analysed by the k_0 -instrumental neutron activation analysis and the activation constant method for 34 elements (Al, As, Ba, Ca, Ce, Co, Cr, Cs, Dy, Eu, Fe, Ga, Hf, K, La, Mg, Mn, Na, Nd, Rb, Ru, Sb, Sc, Se, Sm, Sr, Ta, Tb, V, Yb, Zn, Zr, Th and U). The analysis methodology was discussed with important sources of nuclear and fission product interferences. The important components of uncertainties identified were the k_0 -factor, Q_0 -factor, detector efficiency and counting statistics. The methodology was validated by analyzing the IAEA-S-7 (soil) and IAEA-SL-1 (lake sediment) reference materials. The mass fraction data was explored by principal component analysis. Measured elemental mass fractions were compared with the similar data from other locations of the world. It was shown that anthropogenic activities have little influence on the elemental distribution in the sediment.

Keywords Hunza River · Sediment · k_0 -INAA · Activation constant · MNSR

M. Wasim (✉) · S. Iqbal · M. Arif
Chemistry Division, Pakistan Institute of Nuclear Science and Technology, P.O. Nilore, Islamabad, Pakistan
e-mail: wasim1968@gmail.com

M. Ali
Department of Physics, Karakoram International University, Gilgit, Pakistan

Introduction

Sediment is a particulate matter that transports by the flow of air, water or glaciers and eventually settles down as deposits. Beach sands and river deposits are examples of sediments. In rivers, lakes and oceans, sediments are most often transported by water. It creates river bed, which preserves its own history that is the direction and magnitude of water flow, parent rock lithology and other factors such as environmental pollution. Natural processes responsible for the formation of sediments can be altered by anthropogenic activities. Many man-made materials enter into water bodies through atmospheric deposition, runoff from land, or direct discharge into the water. Energy and mineral consumption by humans is the main cause of contamination of the biosphere. Under certain conditions the contaminants in the bottom sediments may be released back into water and enter into the food chain. Elements are transferred from soil/sediments to surface water to aquatic biota to human. These contaminants may pose a risk to environment on a large scale and hence need to be monitored at regular intervals. Anthropogenic sources of trace elements in sediments are mostly associated with mining of coal, ores and with discharge of municipal waste into river bodies.

The mass fractions of different elements in sediment indicate the level of geochemical or pollution related changes in a water body. Thus, the analysis of sediments can aid in reconstructing its history, in understanding human impact on the ecosystem [1, 2], and in suggesting possible remedial strategies. This information can also be used for modelling different processes [3]. In past, many elemental analysis techniques have been employed for the exploration of sediments. Among these, the X-ray fluorescence spectrometry [4, 5] and instrumental neutron

activation analysis (INAA) have been widely applied [6, 7]. INAA is one of the most suitable methods for geological and environmental samples due to its multielement capability, milligram sample size requirement and freedom from contamination. INAA with semi-absolute methods adds another advantage whereby almost all radionuclides in a spectrum can be quantified; thus extending the range of elements. For this reason k_0 -instrumental neutron activation analysis (k_0 -INAA) has been used extensively for sediment analysis [8, 9]. Another semi-absolute method known as “activation constant (AC) method” [10, 11] also produces accurate results for reactors which show good neutron flux reproducibly such as miniaturized neutron source reactor (MNSR). In our study these two methods of standardization have been applied for the determination of elemental mass fraction in sediments collected along Hunza River in Central Karakorum, Pakistan. This river is an important source of water for Pakistan. To this date, no literature has been cited on the distribution of elements in the Karakoram river system. This paper attempts to collect this information for the first time.

Experimental

Sampling area

Hunza River basin lies in the high Karakoram Range within longitudinal from 74° 02' to 73° 03' and latitudinal from 35° 54' to 37° 05' in the northern territory of Pakistan [12]. In the west it borders by Gilgit River basin, in the north by Afghanistan and China, and in the south by Shigar and Indus River basins. The small portion in the northeast of this basin drains in the Chinese territory. Most of the terrain of the basin is in the elevation range of about 1,500 m above sea level (ASL) to more than 7,500 m ASL. The basin occupies an area of 16389.4 sq. km out of which 87.5 % contributes to Hunza River flow. The glacier cover of the basin is about 4677.3 sq.km [13]. Hunza River is one of the main contributor of water to the river system existed in Pakistan. Its water is assumed pollution free because very little human population inhabit along its banks. Most of the time, it flows in gorges at high speed and is characterized by rapids and falls.

Sampling and sample pre-treatment

In January 2007, nine sediment samples were collected from different locations along Hunza River. The sediments were collected from river side and the upper most layer of sediment from 0 to 10 cm depth was obtained with a stainless steel trowel. The sampling points covered almost 100 km along the river. The geographical parameters of the sampling sites are produced in Table 1 and sampling

Table 1 Geographical information of sampling locations

Sample no.	Altitude (m)	Longitude	Latitude	Location name
1	1,744	74°18'15.58"	36°13'59.72"	Chalt
2	1,742	74°18'21.44"	36°12'2.7"	Gowachi
3	1,596	74°17'15.7"	36°06'07.6"	Nomal
4	1,607	74°17'30.55"	36°05'22.67"	Naltar Nalla
5	1,499	74°22'59.46"	35°55'46.36"	Danyore Nalla
6	1,452	74°18'31.95"	35°55'25.32"	Chinar Bagh
7	1,518	74°24'6.14"	35°53'13.6"	Danyore
8	1,528	74°29'26.28"	35°54'9.34"	Bagrot Nalla
9	1,365	74°29'4.12"	35°52'12.79"	Jalal Abad

locations are depicted in Fig. 1. Among nine samples, five were obtained from the main stream, while four samples were taken from different tributaries entering into the river. Sampling along the river was difficult due to accessibility issues. All samples were collected in clean polyethylene bottles and kept tightly closed. Care was taken to avoid any contamination during and after the sampling [14]. All samples were first air dried and then kept in oven at 105 °C to remove any water content left. Later, all sample were grinded in ball mill for at least 1 hour.

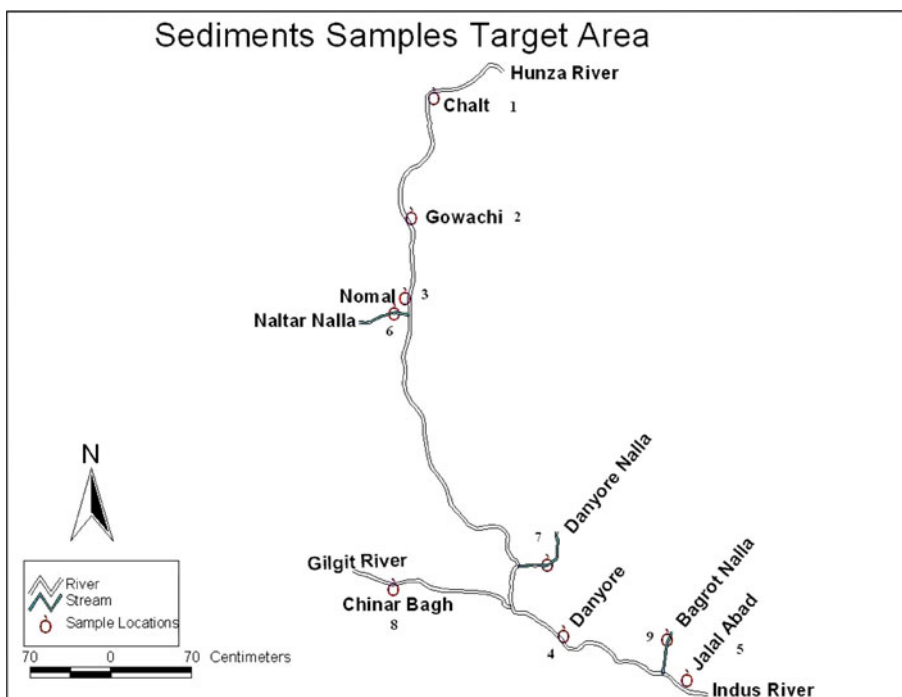
Instrumentation

Each sample weighing up to 150–250 mg was packed inside a polyethylene rabbit along with the Au/Zr monitors [15]. The irradiation was done at Pakistan Research Reactor (PARR-2), which is a MNSR having a nominal thermal neutron flux of $2 \times 10^{12} \text{ cm}^{-2} \text{ s}^{-1}$. After irradiation the samples were transferred to pre-weighed clean polyethylene capsules for counting. The gamma-ray spectra were acquired using a p-type coaxial HPGe detector (Eurisy Measures, France). It is coupled through a 570 ORTEC made spectroscopy amplifier to Trump PCI, 8 k ADC/MCA card with GammaVision-32 ver. 6 Software (ORTEC, USA). The detector has 60 % relative efficiency and FWHM of 2.04 (measured) at 1,332 keV. In spectrum processing, the nuclide identification and quantification were performed using *GammaLab* software [16]. Full peak efficiency calibration of the detector was done for different detector to source geometries using ^{241}Am , ^{133}Ba , ^{137}Cs , ^{60}Co and ^{152}Eu point calibration sources [17].

Methods

In this study, two semi-absolute standardization methods of NAA were employed. These include the k_0 -INAA and the

Fig. 1 Sample locations along Hunza River



AC method. In k_0 -INAA, the thermal to epithermal neutron flux ratio (f) and epithermal flux shape factor (α) are determined for the irradiation channel. The f and α values were determined using Al-0.1 % Au wire (IRMM-530RC, Belgium, Geel) and ZrO_2 (99.99 %, Aldrich, Wisconsin) powder. The f and α were determined for A2 irradiation channel of PARR-2 using “bare triple monitor method” and their values were found as 21.5 and -0.0321 respectively [17, 18]. All the recommended $k_{0,Au}$ factors and nuclear data were taken from the literature [19].

Using k_0 method, the concentration (ρ) of an element “ a ” is calculated as:

$$\rho_a = \frac{A_{sp,a}}{A_{sp,Au}} \frac{1}{k_{0,Au}} \frac{f + Q_{0,Au}(\alpha)}{f + Q_{0,a}(\alpha)} \frac{\epsilon_{p,Au}}{\epsilon_{p,a}} \quad (1)$$

where A_{sp} is the specific activity and is calculated as

$$A_{sp} = \frac{N_p}{wt_m SDC} \quad (2)$$

where N_p is the peak area, w the mass of element, t_m the measurement time, S the saturation factor $[1 - e^{-\lambda t_{irr}}]$ for t_{irr} irradiation time, D the decay factor $e^{-\lambda t_d}$ for t_d decay time and C is the counting factor $[(1 - e^{-\lambda t_m})/\lambda t_m]$. Further details about the k_0 -INAA implementation can be found in our previous work [17]. Similarly, activation constants were obtained from our previous publication [11].

In spectrum processing, several types of interferences are encountered. Usually, geological materials require correction for nuclear reaction by fast neutrons such as (n,p) and (n, α) and fission products produced by ^{235}U [20].

Both types of corrections were applied on the final mass fraction data.

Results and discussion

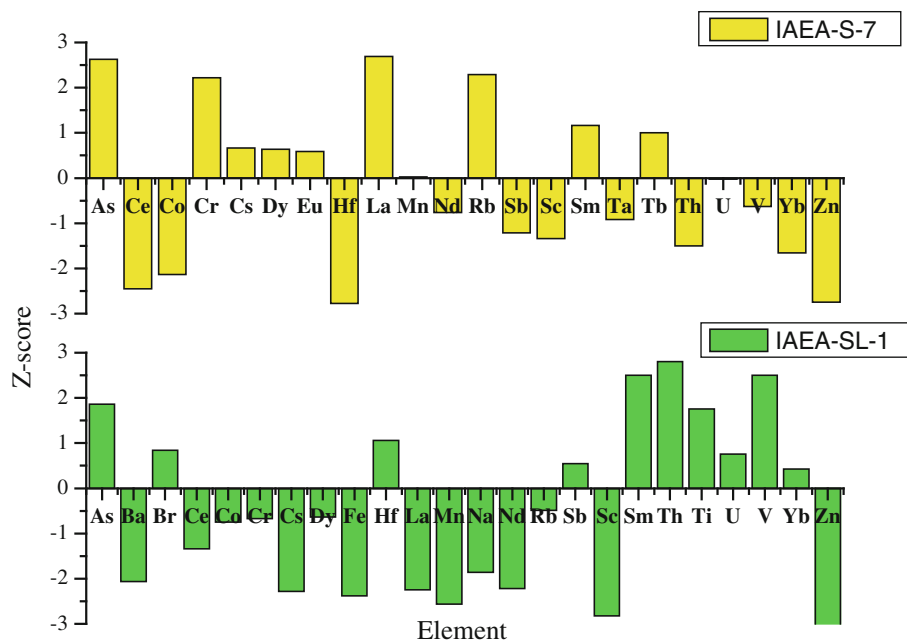
In this study, three irradiations for 3 min, 10 min and 5 h were required for the determination of 38 elements in sediment samples and two reference materials i.e., IAEA-S-7 (soil) and IAEA-SL-1 (lake sediment). The nuclear data for these determinations can be found in our previous studies [15, 21]. Reference materials were analysed for the assessment of experimental accuracy. The results of IAEA-S-7 and IAEA-SL-1 are presented in the form of Z-score in Fig. 2. In this figure all elements are within ± 3 Z-score except for Zn in IAEA-SL-1, which is due to error introduced by the multiplet at 1,115 keV. The Z-score was calculated as

$$Z = \frac{(x_i - x_{ref})}{\sigma_{ref}} \quad (3)$$

where x_i is the measured mass fraction, x_{ref} is the reference mass fraction and σ_{ref} is the reference uncertainty in reference mass fraction for element i . Z-scores for IAEA-S-7 were equally distributed in positive and negative values, while for IAEA-SL-1 there were slightly more negative values. This could be due to variation in flux parameters during the irradiation of IAEA-SL-1.

In this study, Ca and Eu were quantified by the AC method, while rest of the elements was measured by the

Fig. 2 Z-score plots of IAEA-S-7 and IAEA-SL-1, showing that all elements are within ± 3 Z-score except Zn in IAEA-SL-1



k_0 -INAA standardization. Many elements have multiple stable isotopes which may produce more than one radionuclide upon irradiation. In our study, eight elements were determined using two different radionuclides including Ba (^{131}Ba , ^{139}Ba), Br (^{80}Br , ^{82}Br), Ce (^{141}Ce , ^{143}Ce), Eu (^{152}Eu , $^{152\text{m}}\text{Eu}$), Sb (^{122}Sb , ^{124}Sb), Sr (^{85}Sr , $^{87\text{m}}\text{Sr}$), Yb (^{169}Yb , ^{175}Yb) and Zn (^{65}Zn , $^{69\text{m}}\text{Zn}$). The resultant mass fraction was calculated using simple arithmetic average of the two values from two radionuclides. The final mass fractions are based on the average of 3–7 independent measurements i.e., irradiating samples 3–7 times.

In this study, three types of interferences were observed including spectral interferences, nuclear reaction based interferences and interferences by fission products of ^{235}U . All these interferences were handled by our software *GammaLab* [16]. Spectral interferences are resolved during nuclide identification step, while nuclear reaction and fission products are corrected after the analysis is completed. In the analysis of sediment samples, the most significant correction was required for the $^{27}\text{Al}(n,p)^{27}\text{Mg}$ reaction. The other nuclear reactions with more than 0.1 % correction included $^{54}\text{Fe}(n,\alpha)^{51}\text{Cr}$ and $^{88}\text{Sr}(n,p)^{88}\text{Rb}$ reactions. The peak areas of ^{141}Ce , ^{140}La , ^{147}Nd , ^{103}Ru and ^{95}Zr were corrected for the contribution of fission products. The fission correction factors in $\mu\text{g}/\mu\text{g}$ of uranium for ^{141}Ce , ^{140}La , ^{147}Nd , ^{103}Ru and ^{95}Zr were 0.28, 0.0025, 0.22, 0.123 and 9.3 respectively. It should be noted that fission correction factors for ^{140}La , ^{103}Ru are decay time dependent. After making appropriate corrections, the mass fractions of different elements obtained for 9 samples are presented in Table 2.

In k_0 -INAA, the important sources of uncertainty included the k_0 -factor, Q_0 -factor, efficiency, weight and counting statistics. In our study, all the spectra were acquired with less than 5 % dead time. Pulse pile-up corrections were applied to all of them. True coincidence correction was not required because the sample to-detector distance was more than 15 cm in all countings. All mass fractions were based on arithmetic average of individual values. Uncertainties were estimated following the “guide to the expression of uncertainties in measurement” (GUM) [22]. According to the GUM, the total expanded uncertainty contains statistically evaluated uncertainties (type A uncertainty) and uncertainties based on relevant information available (type B uncertainty). In our study, the type A uncertainties were from detector efficiency, weight of sample, peak areas and f value. The type B uncertainties included uncertainties in half-life, Q_0 -factor, k_0 -factor, α value and gold mass fraction (1.2 % from IRMM certificate). Uncertainty in α was taken as 10 % after the recommendations of Robouch et al. [23]. The uncertainties in k_0 - and Q_0 -factors for gold were zero by definition. Before combining, all uncertainties were converted to standard uncertainties.

The elemental mass fraction distribution in sediment samples can be grouped as;

Elements with mass fraction >0.1 %: Al, Ca, Fe, K, Mg, and Na

Elements with mass fraction <0.1 % but >1 mg kg^{-1} : As, Ba, Ce, Co, Cr, Cs, Dy, Eu, Ga, Hf, La, Mn, Nd, Rb, Ru, Sc, Sm, Sr, Th, U, V, Yb and Zn

Elements with mass fraction <1 mg kg^{-1} : Sb, Ta and Tb

Table 2 Elemental mass fraction ($\mu\text{g g}^{-1}$) in 9 sediment samples with uncertainties at $\pm 1\sigma$

Element	Mass fraction ($\mu\text{g g}^{-1}$)								
	Sample 1	Sample 2	Sample 3	Sample 4	Sample 5	Sample 6	Sample 7	Sample 8	Sample 9
Al (%)	7.21 ± 0.64	4.19 ± 0.30	7.87 ± 0.70	12.51 ± 3.05	8.94 ± 2.18	8.27 ± 2.01	7.86 ± 0.69	9.59 ± 0.85	7.10 ± 0.64
As	21.9 ± 1.6	32.5 ± 2.3	7.2 ± 0.5	1.5 ± 0.1	1.2 ± 0.1	51.6 ± 4.7	15.2 ± 1.1	55.7 ± 4.2	10.9 ± 0.9
Ba	402 ± 22	380 ± 30	380 ± 18	106 ± 7	97 ± 6	205 ± 15	350 ± 21	68 ± 4	338 ± 20
Ca (%)	4.98 ± 0.44	6.11 ± 0.52	4.26 ± 0.40	4.49 ± 0.40	4.28 ± 0.36	5.75 ± 0.48	4.24 ± 0.41	7.24 ± 0.51	4.77 ± 0.41
Ce ^a	69.3 ± 12.5	199.7 ± 34.4	78.1 ± 10.0	46.5 ± 9.0	24.8 ± 4.5	22.0 ± 3.9	99.4 ± 17.4	24.9 ± 4.3	108.8 ± 19.7
Co	7.5 ± 0.6	11.0 ± 0.8	6.1 ± 0.5	19.5 ± 1.5	12.0 ± 0.9	27.4 ± 2.2	6.7 ± 0.5	23.5 ± 1.9	8.5 ± 0.7
Cr ^c	37 ± 3	56 ± 4	31 ± 2	67 ± 5	55 ± 4	248 ± 22	38 ± 3	112 ± 8	44 ± 3
Cs	3.53 ± 0.31	3.83 ± 0.32	3.34 ± 0.30	0.85 ± 0.08	0.42 ± 0.04	1.36 ± 0.12	2.66 ± 0.24	1.85 ± 0.16	2.64 ± 0.24
Dy	4.28 ± 0.42	2.55 ± 0.25	3.34 ± 0.27	3.12 ± 0.26	3.11 ± 0.25	3.67 ± 0.30	4.11 ± 0.47	3.31 ± 0.25	4.70 ± 0.45
Eu	1.02 ± 0.08	1.09 ± 0.08	1.51 ± 0.17	2.58 ± 0.30	1.28 ± 0.12	2.63 ± 0.30	1.11 ± 0.08	1.61 ± 0.18	1.85 ± 0.19
Fe (%) ^b	2.27 ± 0.17	3.29 ± 0.24	1.81 ± 0.14	6.88 ± 0.51	3.30 ± 0.24	7.45 ± 0.54	2.02 ± 0.15	6.86 ± 0.52	2.35 ± 0.18
Ga	13.0 ± 1.1	14.2 ± 1.1	–	–	13.9 ± 1.1	–	11.4 ± 0.8	–	17.0 ± 1.2
Hf	6.16 ± 0.49	17.44 ± 1.25	3.28 ± 0.28	3.30 ± 0.28	1.50 ± 0.12	1.53 ± 0.13	3.33 ± 0.24	2.14 ± 0.17	9.68 ± 0.74
K (%)	1.70 ± 0.23	1.75 ± 0.14	1.89 ± 0.24	0.79 ± 0.11	0.94 ± 0.08	0.74 ± 0.10	1.85 ± 0.25	0.77 ± 0.12	1.59 ± 0.22
La ^a	30.6 ± 2.7	85.6 ± 39	38.0 ± 3.1	17.4 ± 1.5	10.4 ± 0.9	8.7 ± 0.7	45.1 ± 3.3	12.0 ± 1.0	39.6 ± 3.6
Mg (%) ^b	1.13 ± 0.22	1.81 ± 0.20	1.11 ± 0.24	1.52 ± 0.67	2.71 ± 0.33	2.70 ± 0.71	1.39 ± 0.25	1.16 ± 0.26	1.39 ± 0.24
Mn (%) ^{b,c}	0.04 ± 0.01	0.06 ± 0.01	0.04 ± 0.01	0.1 ± 0.02	0.08 ± 0.01	0.11 ± 0.02	0.04 ± 0.01	0.09 ± 0.02	0.05 ± 0.01
Na (%) ^{b,c}	1.69 ± 0.19	1.85 ± 0.14	1.90 ± 0.20	2.44 ± 0.30	2.57 ± 0.28	1.90 ± 0.23	1.78 ± 0.19	1.55 ± 0.18	1.76 ± 0.19
Nd ^a	31.1 ± 2.5	84.0 ± 5.9	38.9 ± 2.8	26.5 ± 2.2	9.6 ± 0.7	9.7 ± 0.8	31.6 ± 2.3	11.9 ± 0.9	43.8 ± 3.7
Rb ^b	87.2 ± 6.3	84.7 ± 6	83.6 ± 6.3	21.2 ± 1.6	22.6 ± 1.7	28.2 ± 2.2	77.6 ± 5.7	30.5 ± 2.2	66.9 ± 5.0
Ru ^a	9.7 ± 0.9	24.2 ± 1.7	17.3 ± 1.5	5.4 ± 0.4	3.0 ± 0.2	5.4 ± 0.4	15.9 ± 1.3	3.9 ± 0.3	13.2 ± 1.1
Sb ^a	0.47 ± 0.08	0.59 ± 0.09	0.40 ± 0.09	0.15 ± 0.03	0.16 ± 0.04	0.86 ± 0.13	0.45 ± 0.07	0.94 ± 0.13	0.42 ± 0.07
Sc	9.94 ± 0.90	12.71 ± 1.16	7.20 ± 0.66	21.10 ± 1.84	17.73 ± 1.52	27.38 ± 2.41	8.54 ± 0.74	28.07 ± 2.46	11.52 ± 1.04
Se	–	–	–	–	–	2.44 ± 0.18	–	1.29 ± 0.11	–
Sm	7.85 ± 0.59	11.18 ± 0.77	4.93 ± 0.32	3.71 ± 0.27	2.89 ± 0.19	2.74 ± 0.18	6.64 ± 0.42	3.17 ± 0.21	6.77 ± 0.48
Sr	328 ± 27	340 ± 26	390 ± 25	418 ± 26	668 ± 46	559 ± 62	338 ± 26	401 ± 45	390 ± 20
Ta	1.02 ± 0.06	1.16 ± 0.07	0.84 ± 0.06	0.78 ± 0.06	0.15 ± 0.01	0.23 ± 0.02	0.89 ± 0.05	0.30 ± 0.02	1.36 ± 0.09
Tb	0.73 ± 0.05	1.73 ± 0.10	0.55 ± 0.03	0.67 ± 0.05	0.50 ± 0.03	0.47 ± 0.03	0.64 ± 0.04	0.57 ± 0.04	0.96 ± 0.06
Th	30.70 ± 2.64	161.91 ± 10.17	17.14 ± 1.32	6.39 ± 0.56	2.47 ± 0.18	3.31 ± 0.28	16.55 ± 1.12	3.49 ± 0.23	28.76 ± 2.03
U	3.50 ± 0.29	6.01 ± 0.37	1.85 ± 0.14	–	0.78 ± 0.05	0.52 ± 0.04	2.05 ± 0.17	–	5.16 ± 0.42
V (%) ^{b,c}	65 ± 6	54 ± 6	68 ± 7	65 ± 6	66 ± 7	259 ± 56	149 ± 27	253 ± 75	226 ± 20
Yb	2.35 ± 0.19	7.42 ± 0.52	2.80 ± 0.28	1.69 ± 0.15	1.65 ± 0.14	1.95 ± 0.16	1.91 ± 0.16	1.79 ± 0.14	3.04 ± 0.26
Zn	46 ± 4	59 ± 5	43 ± 4	81 ± 7	62 ± 5	85 ± 7	45 ± 4	87 ± 7	49 ± 4
Zr ^a	375 ± 35	1148 ± 83	205 ± 19	163 ± 12	112 ± 9	–	281 ± 25	–	531 ± 44

^a Corrected for fission product formed by ²³⁵U(n,f) reaction

^b Corrected for (n,p) reaction

^c Corrected for (n,α) reaction

The results of elemental mass fraction were explored further by applying principal component analysis (PCA) [24, 25]. It is a multivariate data exploration technique, which is usually carried out by exploring scores and loading plots. Figure 3 is the scores plot of principal component 3 (PC3) versus PC1. It shows samples in four distinct clusters:

- Cluster 1: sample 2
- Cluster 2: samples 1, 3, 4 and 5
- Cluster 3: samples 6 and 7
- Cluster 4: samples 8 and 9

Similarly, Fig. 4 is the loadings plot of PC3 versus PC1, which shows distribution of elements. It illustrates that

elements are distributed in different groups. Elements close to each other presents high correlation coefficient and indicate a common origin. On comparing Fig. 3 with Fig. 4, it reveals that the sediment samples 1–5, all collected from the main stream are having high mass fractions of rare earth elements (REE). In fact the highest quantities of REE in sample 2 indicate a possible source of rare earth mineral in the vicinity. All the samples collected from tributaries (samples 6–9) show high mass fractions of Al, Fe, Mg, Sc, V and Zn, which indicates their source as crustal elements.

Average mass fractions of major elements (Al, Ca, Fe, K, Mg and Na) in samples were compared with those from other places of the world and the comparison is presented

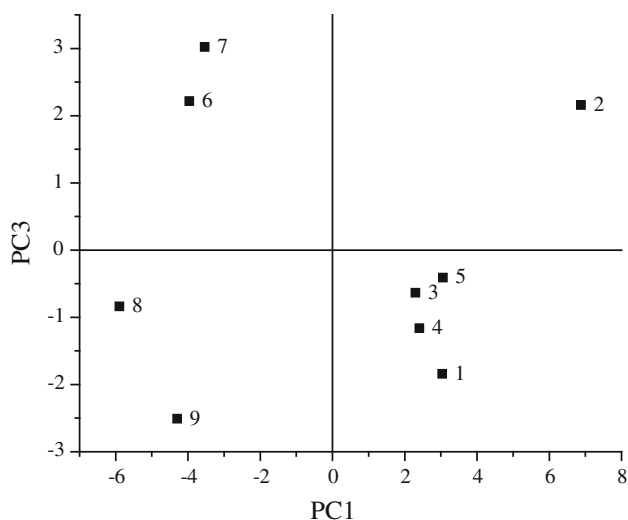


Fig. 3 Scores plot of PC3 versus PC1, showing distribution of samples in four clusters

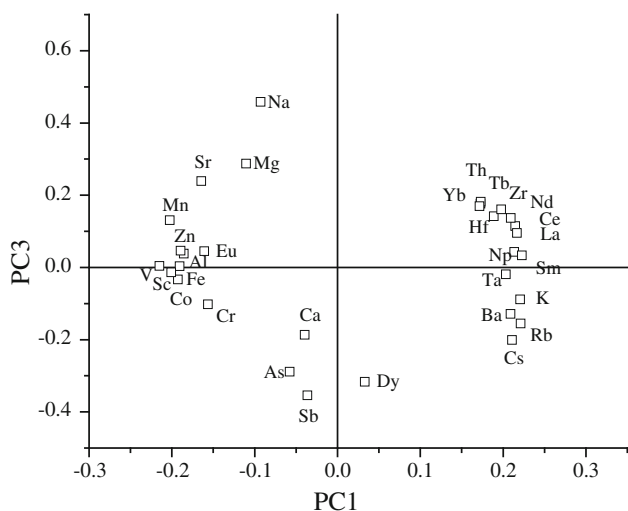


Fig. 4 Loadings plot of PC3 versus PC1, showing relationship among elements

in Table 3. It can be observed that Ca and Na are highest in the Hunza River sediment than the average mass fraction for the Indian, world and surficial rocks. The average mass fraction of Al, Fe and Mg were higher in the Hunza River sediment than those in the Indian and the surficial rocks but lower than the world average mass fractions. The average mass fraction of K in Hunza River sediments was similar to those found at other locations. The data exhibits an enrichment of As at sites 1, 2, 8 and 9. Arsenic is usually associated with lead and copper ores from trace to 2–3 % and with gold ores up to 11 % [26]. The presence of As in these samples need more investigation to ascertain its source properly. The enrichment of Hf, I, Th and Zr at site 2 and Se at sites 8 and 9 was also observed.

Table 3 Mass fraction of major elements (in wt%) in the Hunza River sediments in comparison to the Indian [26] and World river sediment averages [27] and surficial rocks [27]

Element	Hunza average	Indian average	Surficial rocks	World average
Al	8.2	5.0	6.9	9.4
Fe	4.0	2.9	3.6	4.8
Mg	1.66	1.47	1.64	1.18
Ca	5.13	2.46	4.50	2.15
Na	1.94	–	1.42	0.71
K	1.34	1.21	2.44	1.42

REE are characterized by a single oxidation state (+3) except for Ce and Eu, which have additional valences. REE are important geological tracers for the modelling of geochemical processes. Our samples have been characterised with eight REE having mass fractions in the order: Ce > La > Nd > Sm > Dy > Yb > Eu > Tb. A comparison of mass fractions of REE found in our study, after excluding sample 2, with the world average crustal composition [27] shows that La, Ce, Nd and Sm were higher in the Hunza River main stream samples. In tributary samples, La, Ce, Nd, Sm and Yb were lower than the world crustal values. The mass fractions of Eu and Dy were higher in the tributary samples, while mixed trend was shown by these elements in the main stream samples. Elements Tb and Yb exhibited mixed trend in the main stream and tributary samples. The ratio of the light rare earth elements (LREE) to the higher rare earth elements (HREE) was about 20 for the main stream samples and about 8 for the sediments collected from tributaries samples. A Chondrite normalised distributions of REE found in the mainstream and tributary samples are presented in Figs. 5 and 6 respectively. Reference values for REE in Chondrite were taken from Haskin et al. [28, 29] as La: 0.332, Ce: 0.876, Nd: 0.6, Sm: 0.183, Eu: 0.0685, Tb: 0.047, Dy: 0.317 and Yb: 0.207.

The profiles in Fig. 5 show enrichment in the LREE (La, Ce, Nd, Sm) and a depletion in HREE (Eu, Tb, Dy, Yb), which indicates the origin of REEs in the sediment samples from the lithosphere and not from anthropogenic activities. Tributary samples (Fig. 6) exhibited a positive europium anomaly. The Eu in +2 oxidation state has size similar to Ca^{+2} and in reducing magma it substitutes for calcium. Europium enrichment or depletion is attributed towards its tendency to be incorporated into plagioclase over other minerals. If a magma crystallizes stable plagioclase, most of the Eu will be incorporated into this mineral causing a higher than expected concentration of Eu in the mineral versus other REE in that mineral. A comparison of REE in sample 2 shows ratio of mass fractions in our sample to the world average crustal values as: 8.3 (La), 3.4 (Ce),

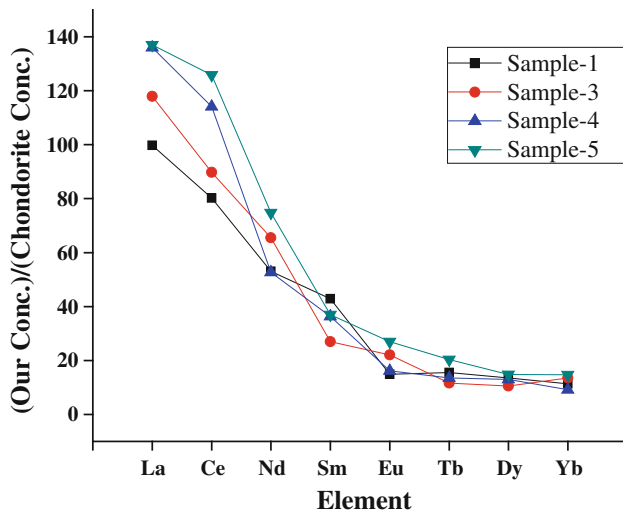


Fig. 5 Chondrite normalized mass fractions of REE in the main stream sediments (locations 1, 3, 4, 5). Sample 2 exhibits the similar trend but not shown here due to scale problem

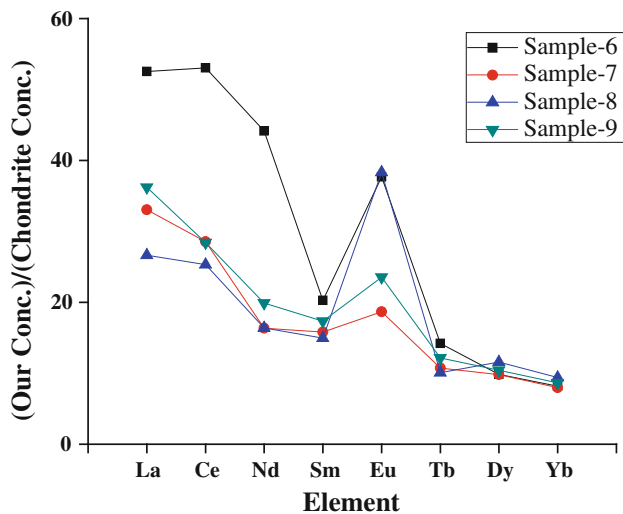


Fig. 6 Chondrite normalized mass fractions of REE in the tributaries sediments showing Eu anomaly (samples: 6, 7, 8, 9)

3.0 (Nd), 2.4 (Sm), 0.9 (Eu), 2.9 (Tb), 0.9 (Dy) and 3.4 (Yb). It indicates an enrichment of La, Ce, Nd, Sm, Tb and Yb at site 2.

Conclusions

In this study the application of INAA with k_0 -standardization and AC methods has determined the mass fractions of 34 elements. This proves semi-absolute standardizations suitable for the characterization of sediment samples. These elements can be quantified using the analysis scheme with three irradiations (3 min, 10 min and 5 h) at a low

power research reactor. Spectrum processing requires corrections for spectral interferences and for the contribution from nuclear reactions and fission products. With the help of PCA it was found that samples from different origin can be differentiated on the basis of elemental concentrations. A comparison of REE with the world average crustal mass fraction shows that at one location, the REE in Hunza River was quite high, which indicates the possible presence of REE mineral in the area. Since there is not much anthropogenic activity and inhabitants along the Hunza River, the physical weathering process is considered as a major factor for the distribution of trace and REE in the sediment.

References

1. Araújo MF, Valério P, Jouanneau J-M (1998) Heavy metal assessment in sediments of the Ave river basin (Portugal) by energy-dispersive X-ray fluorescence spectrometry. X-ray spectrom 27:305–312
2. Crespi VC, Genova N, Tositti L, Tubertini O, Bettoli G, Oddone M, Meloni S, Berzero A (1993) Trace elements distribution in Antarctic sediments by neutron activation analysis. J Radioanal Nucl Chem Artic 168:107–114
3. Loyland SM, LaMont SP, Herbison SE, Clark SB (2000) Actinide partitioning to an acidic, sandy lake sediment. Radiochim Acta 88:793–798
4. Tejada S, Zarazúa-Ortega G, Avila-Pérez P, García-Mejía A, Carapia-Morales L, Diaz-Delgado C (2006) Major and trace elements in sediments of the upper course of Lerma River. J Radioanal Nucl Chem 270:9–14
5. Benyaich F, Makhtari A, Torrisi L, Foti G (1997) PIXE and XRF comparison for applications to sediments analysis. Nucl Instrum Method Phys Res Sect B 132:481–488
6. Akyuz T, Mukhamedshina N, Akyuz S, Sari E, Mirsagatova AA (2007) Toxic and trace element analysis of surface sediments from the Gulf of Saros by INAA and XRF methods. J Radioanal Nucl Chem 273:747–751
7. Silva PSC, Mazzilli BP, Fávoro DIT (2006) Distribution of radionuclides and elements in Cubatão River sediments. J Radioanal Nucl Chem 269:767–771
8. Smodis B, Jacimovic R, Medin G, Jovanovic S (1993) Instrumental neutron activation analysis of sediment reference materials using the k_0 -standardization method. J Radioanal Nucl Chem Artic 169:177–185
9. Ferreira JR, Fernandes EAN, França EJ, Tavares GA, da Silva NC, Taddei MHT (2006) Rare earth elements in sediment profiles from marginal lagoons of the Moji-Guaçu River basin, Brazil. J Radioanal Nucl Chem 270:15–20
10. Bergerioux C, Kennedy G, Zikovskiy L (1979) Use of the semi-absolute method in neutron activation analysis. J Radioanal Chem 50:229
11. Wasim M, Arif M, Zaidi JH (2011) Determination of the activation constants for miniature neutron source reactor (MNSR) by linear least squares regression. Radiochim Acta 99:59–63
12. Shroder JF (1992) Himalaya to the Sea: geomorphology and the quaternary of Pakistan in the regional context. Routledge, London
13. Goudie AS, Brunsten D, Collin DN, Derbyshire E, Ferguson RI, Hashmet Z, Jones DKC, Perrott FA, Said M, Waters RS, Whalley WB (1984) The geomorphology of Hunza valley, Karakoram

- mountains, Pakistan. In: Proceedings of the international Karakoram project, Cambridge University Press, Cambridge
14. IAEA-TECDOC-1360 (2003) Collection and preparation of bottom sediment samples for analysis of radionuclides and trace elements. IAEA, Vienna
 15. Wasim M, Arif M, Zaidi JH, Fatima I (2008) Quantitative analysis of ancient Chinese ceramic using k_0 -instrumental neutron activation analysis. *Radiochim Acta* 96:863–866
 16. Wasim M (2010) GammaLab: a suite of programs for k_0 -NAA and gamma-ray spectrum analysis. *J Radioanal Nucl Chem* 285:337–342
 17. Wasim M, Zaidi JH, Arif M, Fatima I (2008) Development and implementation of k_0 -INAA standardization at PINSTECH. *J Radioanal Nucl Chem* 277:525–529
 18. Simonits A, De Corte F, Hoste J (1975) Single comparator methods in reactor neutron activation analysis. *J Radioanal Chem* 24:31–46
 19. De Corte F, Simonits A (2003) Recommended nuclear data for use in the k_0 standardization of neutron activation analysis. *At Data Nucl Data Tables* 85:47–67
 20. Martinho E (1999) Determination of ^{235}U abundance in uranium by neutron activation on the basis of the molybdenum fission interference. *J Radioanal Nucl Chem* 241:271–276
 21. Wasim M, Arif M, Iqbal S, Daud M (2013) Provisional elemental values for IAEA-sewage sludge by instrumental neutron activation analysis. *Geostand Geoanal Res* 37:87–93
 22. BIPM (2008) Evaluation of measurement data—guide to the expression of uncertainty in measurement. JCGM 100:2008
 23. Robouch P, Arana G, Eguskiza M, Pommé S, Etxebarria N (2000) Uncertainty budget for k_0 -NAA. *J Radioanal Nucl Chem* 245:195–197
 24. Vandeginste BGM, Massart DL, Buydens LMC, Jong SD, Lewi PJ, Smeyers-Verbeke J (1998) Handbook of chemometrics and qualimetrics, part B. Elsevier, Amsterdam
 25. Daud M, Wasim M, Khalid N, Zaidi JH, Iqbal J (2009) Assessment of elemental pollution in soil of Islamabad city using instrumental neutron activation analysis and atomic absorption spectrometry techniques. *Radiochim Acta* 97:117–122
 26. Nyarko BJB, Serfor-Armah Y, Holzbecher J, Osae EK, Akaho EHK, Carboo D, Chatt A (2003) Epithermal instrumental neutron activation analysis for the determination of gold and arsenic in Ghanaian gold tailings using conventional and anti-coincidence counting. *J Radioanal Nucl Chem* 256:253–257
 27. Kabata-Pendias A, Mukherjee AB (2007) Trace elements from soil to human. Springer, Berlin
 28. Haskin LA, Wildeman TR, Haskin MA (1968) An accurate procedure for the determination of the rare earths by neutron activation. *J Radioanal Chem* 1:337–348
 29. Haskin LA, Helmke PA, Paster TP, Allen RO (1971) Rare earths in meteoritic, terrestrial, and lunar matter. NATO conference on activation analysis in geochemistry and cosmochemistry, pp 201–218